ELSEVIER

Sensors and Actuators A 101 (2002) 215–219

SENSORS AND ACTUATORS A PHYSICAL

www.elsevier.com/locate/sna

Nanomechanical resonant structures in silicon nitride: fabrication, operation and dissipation issues

L. Sekaric*, D.W. Carr[1], S. Evoy[2], J.M. Parpia, H.G. Craighead

Cornell Center for Materials Research, Cornell University, Ithaca, NY 14853, USA

Received 8 December 2000; accepted 3 April 2002

Abstract

We report the fabrication of silicon nitride mechanical devices with lateral dimensions as small as 50 nm. The measured resonant frequencies of these devices (8.5–171 MHz) are the highest reported for silicon nitride structures. We have employed both electrostatic and piezoelectric excitation of these structures. We have also studied the effects of thin metal films on dissipation in these structures and found that the absence of these metal coatings results in a three to four times higher quality factor of the structures.

Keywords: Nanomechanics; Silicon nitride; Mechanical quality factor; Dissipation

1. Introduction

Nanomechanical systems have generated great interest in the scientific and engineering communities. Their potential for ultrasensitive sensor applications as transducers for small forces [1], high frequency oscillators for mechanical filters [2], and for mass assays (as both chemical and biological detectors) [3] has also posed new challenges in the studies of the physical properties of these systems. The understanding of the dissipation processes is one of the important issues for a successful application of these systems.

Determining the cause of dissipation in micro and nanomechanical resonators is of current interest [4–9]. The decrease in size of mechanical systems is typically accompanied by a decrease in their mechanical quality factor. Resonators a few orders of magnitude larger than the devices reported here have quality factor values of about 11,000 at room temperature [7]. A further decrease in the quality factor by an order of magnitude can be significant and undesirable for some applications. Our motivation to examine silicon nitride was to study materials, other than silicon, that can be processed by surface micromachining. We are also interested in considering a different chemistry to compare dissipation in different materials. We were able to employ well-developed fabrication processes, such as material deposition and dry etching. Our previous work in silicon resonators [4] indicates that surface losses may dominate in this size scale. In this investigation, we have examined the effects of thin metal layers on the dissipation processes in nanomechanical silicon nitride structures as metal layers can be an integral part of the operation of the devices that are actuated electrostatically. The fabrication technique is similar to that used for fabricating high frequency (380 MHz) silicon mechanical devices [4] and the driving and the detection methods have been widely used, both for electrostatic and inertial operation [4–7,10,11].

2. Fabrication

Starting with a commercially available (1 0 0) single-crystal silicon wafer (as shown in Fig. 1), we grow 400 nm of silicon dioxide by thermal oxidation. We then deposit 230–250 nm of silicon-rich amorphous silicon nitride, by low-pressure chemical vapor deposition (LPCVD). The fabrication approach is similar to that used to make single-crystal silicon devices [4,10,11]. The wafers are patterned using 100 kV electron beam lithography. After the development of a bilayer poly-methylmethacrylate (PMMA) resist, we evaporate 40 nm of Cr and perform a lift-off procedure to make the mask for nitride etching. The nitride is etched using a reactive ion etch in a CF_4–H_2 plasma. After removal of the

* Corresponding author.
E-mail address: ls63@cornell.edu (L. Sekaric).
[1] Present address: Lucent Technologies, Murray Hill, NJ, USA.
[2] Present address: University of Pennsylvania, The Moore School of Electrical Engineering, Philadelphia, PA, USA.

0924-4247/02/$ – see front matter
PII: S0924-4247(02)00149-8

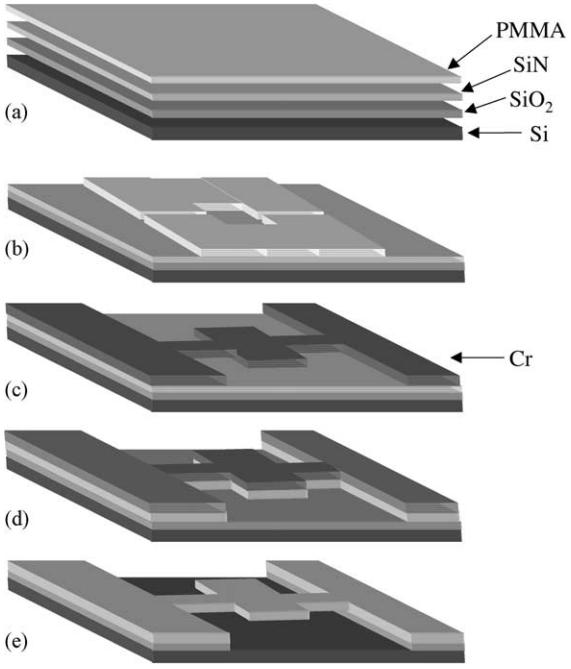

Fig. 1. The fabrication sequence for the devices: (a) bare silicon wafer is oxidized, after which silicon nitride is deposited and PMMA is used as an electron-beam resist layer; (b) PMMA after exposure and development; (c) a metal (Cr) mask is deposited after which some metal is lifted off with the unexposed resist; (d) the remaining mask serves to define the pattern in the silicon nitride using a reactive ion etch; (e) after the mask is removed, the underlying silicon dioxide is etched away resulting in a suspended structure.

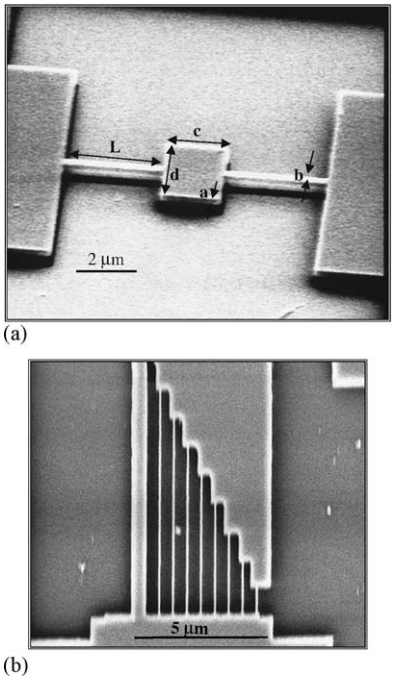

Fig. 2. (a) A scanning electron micrograph of a 2 μm × 2 μm silicon nitride paddle. The supporting rods are 230 nm wide and 3 μm long, and the thickness of the device layer is 240 nm. (b) A scanning electron micrograph of silicon nitride suspended wires. The length of the wires varies from 1 to 8 μm.

Cr mask in O_2 plasma, the devices are released by removing the underlying oxide layer in buffered hydrofluoric acid. Since air-drying causes stiction and significantly reduces the yield, the devices are dried in a critical point dryer [12]. After this step, the yield is 98%. After drying, we evaporate 5 nm Cr and 17–20 nm of Au on some of the devices. The resulting structures used for this study are shown in Fig. 2a and b.

3. Experiment

The structures are mounted in a vacuum chamber at pressures ranging from 1×10^{-3} to 50×10^{-3} Torr. The devices are actuated by two different methods: electrostatic and inertial. The electrostatic drive consists of applying an ac drive voltage and a dc bias voltage to the device with the substrate grounded [4,10,11]. The resulting force induces motion at the frequency of the ac drive signal. For the inertial drive, the devices are mounted on a piezoelectric element to which we apply the ac drive voltage. This element responds to the drive frequencies up to about 50 MHz. A Hewlett-Packard ESA-L1500A spectrum analyzer with a tracking output provides the ac signal from 9 kHz to 1.5 GHz for both driving methods. This signal is amplified 50 dB by a radio frequency amplifier. The motion of the devices is detected optically. A He–Ne laser light is focused onto the device which acts as a Fabry–Pérot interferometer [10], and the signal is detected via a New Focus 1601 ac coupled photodetector. The signal from the photodetector is sent to the frequency-sweeping spectrum analyzer. We obtain optical amplitude versus drive frequency response that has a Lorentzian form (Fig. 3). Both the electrostatic drive and interferometric detection have been described in more detail

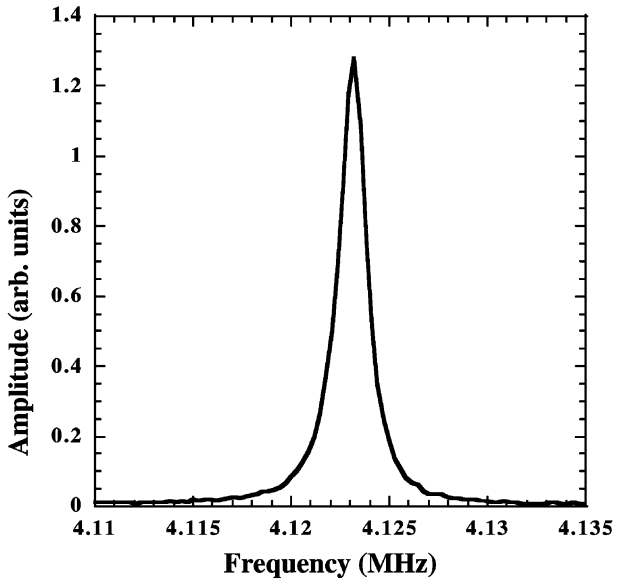

Fig. 3. Resonant response of a paddle device.

(including a schematic representation) in our previous work [10]. The frequency and Q stability are very high for a given structure and any variations we find are from chip to chip due to fabrication non-uniformity.

4. Results and discussion

We previously reported the fabrication and electrostatic operation of similar single-crystal silicon paddles [11] and silicon wires [4]. Here we will provide a comparison with those results to draw conclusions about the differences in the operation of the nitride devices. We use two different driving schemes to actuate the nitride devices. Metallized nitride paddles and wires are driven electrostatically, enabling us to make a comparison with the previously obtained results for similarly metallized single-crystal silicon. Metallized and non-metallized nitride devices are driven inertially, which provides useful information on the contribution of the metal layers in the dissipation processes.

The resonant frequencies for the paddles are in the range 8.5–26 MHz. From the paddle length dependence of the resonant frequency [11], we find that the nitride devices are excited in a vertically translational (flexural) mode of motion; because we were unable to excite any other modes of motion in most structures we will limit our discussion to only the flexural mode. The resonant frequency of this motion is given by:

$$f = \frac{1}{2\pi}\sqrt{\frac{2Ea^2b}{\rho dcL^3}}, \quad (1)$$

where E is the Young's modulus of the material, ρ the density of the material (2860 kg m^{-3} for silicon nitride) and a the thickness of the device, b and L are the width and the length of the supporting beam, c is the length of the paddle and d its width, as noted in Fig. 2a. From Eq. (1) we have determined a Young's modulus for silicon nitride of 1.1×10^{11} Pa. This value is consistent with several values previously reported for thin film LPCVD silicon nitride [13,14]. In order to obtain more information about material-related properties, we compare the results from metallized single-crystal silicon [11] with those for metallized silicon nitride. In Fig. 4a and b, we plot the resonant frequency versus the length of the paddle (d) and versus the length of the supporting rods (L). The power law dependence of the resonant frequency of silicon and silicon nitride devices on the length of the paddle is identical (Fig. 4a). The frequency dependence on the supporting rod length is different for silicon (the power is −1.2) than for silicon nitride (the power is −0.9) as can be seen in Fig. 4b.

We also studied suspended silicon nitride wires (Fig. 2b) fabricated on the same substrate as the paddles, using identical fabrication process. The length of the wires varies from 1 to 8 μm and the width from 50 to 300 nm. The

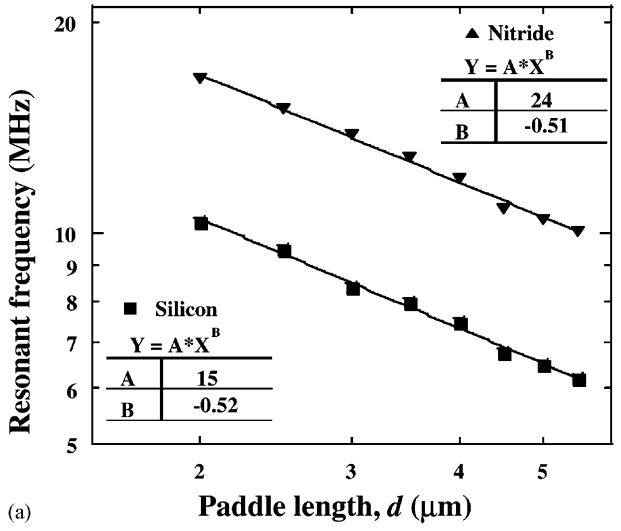

(a)

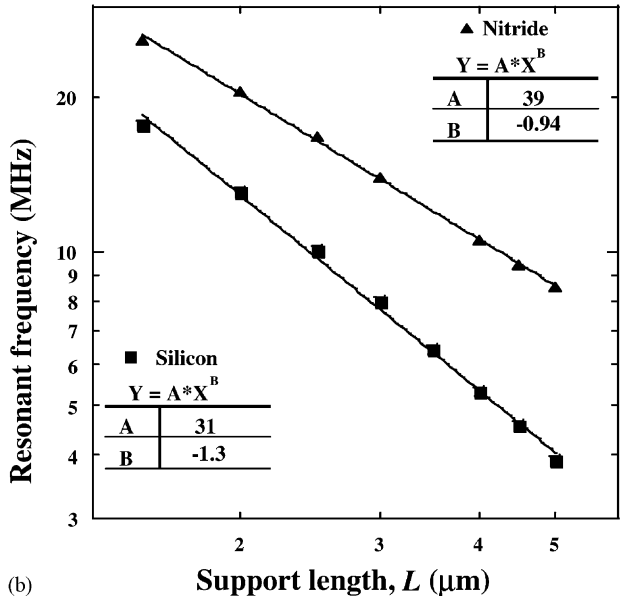

(b)

Fig. 4. (a) Resonant frequency dependence on the length of the paddle (d), where the paddle length varies from 2.0 to 5.5 μm. The supporting beam length is 2.5 μm. Results given are for single-crystal silicon (■) and for silicon nitride (▲). The power law dependence for the two cases is also given and is almost identical. (b) Resonant frequency dependence on the length of the supporting beams (L), where the support length varies from 1.5 to 5.0 μm. The paddle length is 2 μm. The results are for silicon (■) and silicon nitride (▲). The power law dependence is slightly different for the two cases.

measured frequencies of these wires vary from 29 MHz for the longest, 8 μm wire to 171 MHz for the 3 μm long wire and the quality factors are 2000–2500. The frequency dependence on the length of the wires is proportional to $l^{-1.8}$, where l is the length of the wire, as can be seen from Fig. 5. This dependence deviates slightly from the l^{-2} dependence which is the expected dependence for such a system free of tension, and as found for single-crystal silicon wires [4]. We attribute this deviation to the tensile stress

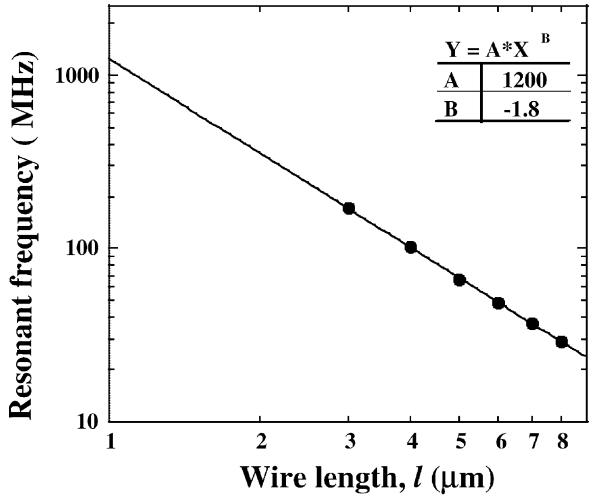

Fig. 5. Resonant frequency dependence on the length of the wire. The power law dependence is also given. The wire is 220 nm thick and 230 nm wide.

found in the nitride, and can be compared to the similar effect it produced in the silicon nitride paddles (Fig. 4b). Using the curvature (wafer bow) method, we find that the LPCVD-grown nitride is under a tensile stress of 172 MPa which might explain the slight difference in the power law for two materials, as can be seen from the following analysis. Resonant frequency of a doubly-clamped beam free of tension is given by:

$$f_i = \frac{k_i^2}{2\pi l^2}\sqrt{\frac{EI}{\rho A}}, \tag{2}$$

where l is the length of the wire, E the Young's modulus of the material, I the second moment of inertia of a rectangular beam, ρ the density of the material and A the cross-section of the beam and $k_i = 4.730$ for the first mode [15]. For a beam under tensile stress (S), we have [15]:

$$f_{iS} = f_i\sqrt{1 + \frac{Sl^2}{k_i^2 EI}}. \tag{3}$$

In the limit of the stress term being small, this correction becomes:

$$f_{iS} = f_i + \frac{S}{8\pi\rho A}\sqrt{\frac{3}{EI(a^2+b^2)}}, \tag{4}$$

where a, b are the cross-sectional dimensions of the wire. In the limit that the stress term is much larger, this correction leads to:

$$f_{iS} = \frac{k_i^2}{2\pi l}\sqrt{\frac{S}{\rho A}}. \tag{5}$$

The resonant frequencies of the silicon nitride wires that we measure do not follow results for a system completely free of tension nor do they seem to be under high tension and we have to conclude that both additional numerical analysis with higher order terms in the earlier expansions (3) and (4) are needed to fully fit the data.

The resonant frequency of these wires is higher that that of the silicon systems of the same dimensions, a result that can be attributed to both the effects of the slightly higher Young's modulus of silicon nitride (relative to about 87 GPa we found in silicon [11]) and the effect of tensile stress, as can be seen from Eq. (3). The resulting increase in the effective structural rigidity also makes it more difficult to actuate the wires and thus, we were not able to detect the motion of the 2 and 1 μm long wires with the existing measurement apparatus (e.g. in silicon [4] we were able to measure the 2 μm wires). Following the linear fit in Fig. 5, we expect the resonance frequency of the shortest wire to exceed 1 GHz. Current modifications to the measurement setup are underway to enable us to detect the motion of the shortest suspended wires.

In order to study the effects of thin metal films on these devices, the inertial method of actuation was used to drive metallized and non-metallized nitride paddles. The resonant frequency was higher only due to the lower mass of the non-metallized devices. Calculating the Young's modulus for the paddles we find a change of 6% in the stiffness due to the metal layer. The main contribution of the metal film appears to be in the mechanism of dissipation. The quality factor values of the non-metallized devices are in the range 2000–4000, which is almost four times higher compared to the quality-factor range of the metallized devices (mostly 500–1000) (Fig. 6). In all of the cases, the driving signal is kept low, so that the amplitude response is linear with the drive.

The results presented indicate that using silicon nitride for the fabrication of nanomechanical systems might be somewhat favorable for several reasons. Since LPCVD nitride is under tensile stress this might contribute to the increased yield in the fabrication by reducing stiction. Also

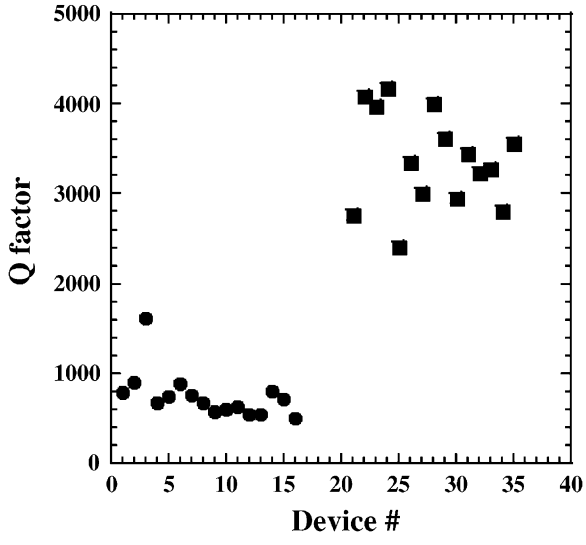

Fig. 6. Quality factor values of silicon nitride paddles for inertially driven, metallized paddles (■) and inertially driven non-metallized paddles (●).

the resonant frequencies are higher than in silicon structures of similar dimensions.

We compared the operation of metallized and non-metallized devices and found that the absence of the metal layer resulted in higher quality factor values. It has been found that in similar silicon nitride structures of thickness less than 2 μm dissipation is not thermoelastic [7], whereas for silicon structures [9] there are calculations which show that it still may be an important loss mechanism at room temperature, but other experimental work, also on silicon structures of comparable geometry and size, has indicated that the dominant losses may be surface-related [4]. No matter what the dominant loss mechanism in this size scale, metal layers seem to add to the losses significantly. Even in larger silicon systems, where thermoelastic dissipation dominates [16], thin metal films are known to contribute significantly to the dissipation. Furthermore, the results obtained from single-crystal silicon systems [4,11] give quality factors (1000–3000) comparable to those of electrostatically driven nitride devices. Since we do not expect identical or even similar dissipation processes in crystalline and amorphous materials, we conclude that metal layers not only significantly contribute, but possibly dominate losses in systems on this size scale, when used in fabrication. Alternative driving schemes as well as different conducting layers (such as doped polycrystalline silicon) should be considered in the case of ceramic NEMS.

5. Conclusion

We fabricated silicon nitride mechanical structures with dimensions as small as 50 nm and obtained an almost perfect yield. These devices have the highest measured resonant frequencies (171 MHz) reported in the literature to date for nitride devices. We also studied the effects of thin metal films on these structures and found that their presence is detrimental even in amorphous-material NEMS on this size scale. Developing new driving schemes which do not require the presence of thin metal films on the actuated elements, such as the piezoelectric drive, could increase the quality factor of these structures significantly, which would make them a more desirable candidate for many sensor applications.

Acknowledgements

This work was supported by the Cornell Center for Materials Research (CCMR), a Materials Research Science and Engineering Center of the National Science Foundation (DMR-0079992). All of the fabrication was performed at the Cornell Nanofabrication Facility, also funded by the National Science Foundation. The authors would like to thank Kevin Yasumura for many useful discussions.

References

[1] J.A. Sidles, J.L. Garbini, K.J. Bruland, D. Rugar, O. Zuer, S. Hoen, C.S. Yannoni, Magnetic resonance force microscopy, Rev. Mod. Phys. 67 (1995) 249.
[2] F.D. Bannon, J.R. Clark, C.T.C. Nguyen, High-Q HF microelectromechanical filter, IEEE J. Solid State Circuits 35 (10) (2000) 1517.
[3] B. Ilic, D. Cazaplewski, H.G. Craighead, P. Neuzil, C. Campagnolo, C. Batt, Mechanical resonant immunospecific biological detector, Appl. Phys. Lett. 77 (2000) 450.
[4] D.W. Carr, S. Evoy, L. Sekaric, H.G. Craighead, Losses in nanometer scale silicon wires, Appl. Phys. Lett. 75 (7) (1999) 920.
[5] K.Y. Yasumura, J.A. Chiaverini, T.W. Kenny, D. Rugar, Thermoelastic dissipation in silicon nitride microcantilevers, in: Proceedings of the 10th International Conference on Solid State Sensors and Actuators, Transducers '99, 1999, p. 564.
[6] K.Y. Yasumura, T.D. Stowe, E.M. Chow, T. Pfafman, T.W. Kenny, D. Rugar, A study of microcantilever quality factor, in: Proceedings of the Solid State Sensor and Actuator Workshop, Hilton Head, 1998, p. 65.
[7] K.Y. Yasumura, T.D. Stowe, E.M. Chow, T.E. Pfafman, T.W. Kenny, B.C. Stipe, D. Rugar, Quality factors in micron and submicron thick cantilevers, J. Microelectromech. S 9 (1) (2000) 117.
[8] R. Lifshitz, M.L. Roukes, Thermoelastic damping in micro- and nanomechanical systems, Phys. Rev. B 61 (8) (2000) 5600.
[9] D.A. Harrington, P. Mohanty, M.L. Roukes, Energy dissipation in suspended micromechanical resonators at low temperatures, Phys. B 284–288 (2000) 2145.
[10] D.W. Carr, H.G. Craighead, Fabrication of nanomechanical systems in single-crystal silicon using silicon on insulator substrates and electron beam lithography, J. Vac. Sci. Technol. B 15 (6) (1997) 2760.
[11] S. Evoy, D.W. Carr, L. Sekaric, A. Olkhovets, J.M. Parpia, H.G. Craighead, Nanofabrication and electrostatic operation of single-crystal silicon paddle oscillators, J. Appl. Phys. 86 (11) (1999) 6072.
[12] G.T. Mulhern, D.S. Soane, R.T. Howe, Supercritical carbon dioxide drying of microstructures, in: Proceedings of the Seventh International Conference on Solid State Sensors and Actuators, Transducers '93, 1993, p. 296.
[13] C.J. Drummond, T.J. Senden, Characterisation of the mechanical properties of thin film cantilevers with the atomic force microscope, Mater. Sci. Forum 189/190 (1995) 107.
[14] L. Kiesewetter, J.-M. Zhang, D. Houdeau, A. Steckenborn, Determination of Young's moduli of micromechanical thin films using the resonance method, Sens. Actuators A 35 (1992) 153.
[15] S. Timoshenko, D.H. Young, W. Weaver, Vibration Problems in Engineering, 4th Edition, Wiley, New York, 1974, pp. 424–454.
[16] X. Liu, E. Thompson, B.E. White Jr., R.O. Pohl, Low-temperature internal friction in metal films and in plastically deformed bulk aluminum, Phys. Rev. B 56 (18) (1999) 11767.